Kinetic Trends in RAFT Homopolymerization from Online Monitoring

Alina M. Alb,[†] Algirdas K. Serelis,[‡] and Wayne F. Reed*,[†]

Physics Department, Tulane University, New Orleans, Louisiana 70118, and Dulux Australia, 1970 Princes Highway, Clayton, Victoria 3168, Australia

Received July 16, 2007; Revised Manuscript Received October 5, 2007

ABSTRACT: Automatic continuous online monitoring of polymerization reactions (ACOMP) was used to follow kinetic trends in the reversible addition−fragmentation chain transfer (RAFT) polymerization of butyl acrylate (BA) in butyl acetate, using 2-{[(dodecylsulfanyl)carbonothioyl]sulfanyl}propanoic acid (DoPAT) as the RAFT agent and 2,2-azobis(isobutyronitrile) as the initiator (AIBN). The goals were to demonstrate the use of ACOMP for RAFT studies and to examine the trend in conversion and evolution of weight-average molar mass M_w and weight-average intrinsic viscosity $[\eta]_w$ for a series of experiments in which the RAFT agent concentration was decreased over a wide range while all the other reaction conditions were held constant; [DOPAT]/[AIBN] ranged from 0 to 2.4. This allowed monitoring the transition from "living"-like behavior in the "controlled radical polymerization" (CRP) regime, where sufficient RAFT agent was used, to the noncontrolled radical polymerization regime as RAFT agent was progressively reduced to zero. The conversion kinetics were found to be essentially zeroeth order in DoPAT, and deviations from living behavior allowed estimates of radical efficiency. The evolution of M_w vs monomer conversion varied dramatically from near-ideal living behavior at high [DoPAT]/[AIBN] to classical radical polymerization behavior at [DoPAT] = 0. All but one experiment showed a nonzero M_w at f = 0, and the conversion behavior of M_w points to transfer and branching side reactions, depending on [DoPAT]. ACOMP should prove to be a useful tool both for fundamental RAFT research and process development.

Introduction

The demand for higher performance and more specialized materials has engendered a strong research focus on living/controlled polymerization reactions (CRP).[1,2] CRP reactions have attracted a lot of attention from various research groups. Their versatility and robustness against impurities, and their compatibility with a large number of monomers and functional groups, combined with the living character that the CRP systems manifest open a new window to the production of novel materials with controlled molecular weight and well-defined structures and architectures. Chain modifications, close control of composition, and, hence, polymer properties[3] are possible due to the long time (hours) between initiation and the end of propagation, compared to a few seconds to form a complete chain in classical radical polymerization.

Among the radical polymerization techniques with living or quasi-living character, the most common by far are (i) nitroxide-mediated radical polymerization (NMP),[4] (ii) atom transfer radical polymerization (ATRP),[5,6] and (iii) reversible addition−fragmentation chain transfer (RAFT) polymerization.[7] These are distinguished from each other on the basis of the mechanism that ensures the living character of the reaction. Thus, NMP is based on reversible termination by coupling, in which the P−ONR_2 bond is cleaved to produce the persistent radical R_2-NO$^\bullet$ and a propagating polymer radical P$^\bullet$, and the ATRP mechanism involves the reversible termination by ligand transfer to a metal complex, whereas in RAFT the living character is achieved by reversible chain transfer. The initial transfer agent in RAFT is a species generally designated as Z−C(=S)S−R which reacts with initiating (I$^\bullet$) or propagating radicals (P$^\bullet$) to give another transfer agent (Z−C(=S)S−I or Z−C(=S)S−P) and a species capable of initiating polymerization (R$^\bullet$).

RAFT is the newest of the major CRP methodologies, and it has rapidly established itself as arguably the most versatile. It has been comprehensively reviewed in recent years.[8−15] A judiciously chosen RAFT agent will allow the controlled polymerization of any monomer to high conversion and almost any predetermined molecular weight. In selecting RAFT agents, the important considerations are that R must have adequate radicofugal and reinitiating ability relative to the monomer being polymerized and that Z (alkyl or aryl in dithioesters; alkylthio in trithiocarbonates; alkoxy or aryloxy in xanthates; disubstituted alkyl- or arylamino, or *N*-heterocyclyl, in dithiocarbamates) must be chosen to impart the proper attenuation of reactivity to the addition and fragmentation reactions of the polymerizing radicals. As with other CRP methods, block copolymers are easily synthesized as well as more complex architectures[15] such as star, dendritic, and brush/comb/graft homopolymers and copolymers.

A large number of RAFT agents have been synthesized to date, and limitless others can be designed to order. The functionality of the R and Z groups of the initial RAFT agent is retained in the final polymer as two end groups which may, if desired, be removed, altered, or used for further functionalization or polymer coupling. Hence, RAFT chemistry is finding widespread use as a nanoengineering tool for stimuli-responsive polymers,[16−20] inorganic composites,[21,22] particle encapsulation and surface modification,[23−31] construction of hollow, core−shell, and functionalized micelles,[32−36] and synthesis of biohybrids such as glycopolymers[37−40] and protein−polymer conjugates.[41,42]

RAFT polymerizations, with the notable exception of those mediated by dithiobenzoates,[13] usually proceed at close to conventional polymerization rates and can be performed in a variety of media with a high degree of compatibility toward a wide range of functionality in monomers, solvents, and initiators. Of particularly profound commercial and environmental sig-

* Corresponding author.
[†] Tulane University.
[‡] Dulux Australia.

10.1021/ma071579p CCC: $40.75
Published on Web 12/15/2007

Scheme 1

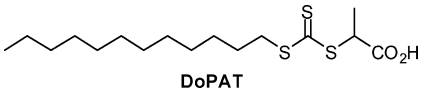

DoPAT

nificance is the facility with which RAFT polymerizations can be conducted in heterogeneous aqueous systems,[43−50] such as dispersions, suspensions, emulsions, and miniemulsions, all of which are processes that are immensely important on an industrial scale.

The goal of the current work is to demonstrate the utility of ACOMP for monitoring RAFT polymerizations and to chart the change in kinetics and molar mass evolution as the concentration of RAFT agent is decreased, and the polymerization mechanisms change from "living" radical type to conventional uncontrolled radical type, while all other reaction conditions are held constant. It is hoped that ACOMP will be generally useful for mechanistic and applied RAFT studies. There are, however, many unresolved mechanistic questions concerning the RAFT process, and an extensive and deep literature exists, including several excellent reviews.[51,52] It is beyond the scope of this work to make comparative mechanistic analyses. Rather, the focus is on the type of comprehensive data that can be obtained and how specific trends in reaction conditions can be followed. An important gap in the current data is that it does not follow the several subspecies present in very small concentration that can profoundly affect rates and equilibrium. Since ACOMP is an evolving method, however, it may be possible to adapt appropriate detectors for such species into the detector train (e.g., EPR, FTIR).

In the current work, the RAFT agent used is the unsymmetrical trithiocarbonate DoPAT (Scheme 1). Trithiocarbonates, symmetrical as well as unsymmetrical, are coming into increasing prominence[8−13,53] because of their generally good kinetic behavior combined with superior resistance to hydrolysis[46] in aqueous media and ease of synthesis. The concentration-dependent rate retardations which sometimes occur in trithiocarbonate-mediated polymerizations, unlike those of dithiobenzoates, are not considered to be particularly severe.[8,11,14,45,54] The few quantitative determinations of chain transfer constants (C_t) for trithiocarbonates[54−57] point to an expectation of relatively high values provided the proper structural considerations are taken into account, and this is borne out by their widely successful application. DoPAT was first introduced for the synthesis of short acrylic acid macroRAFT agents as precursors to amphiphilic diblocks for use in emulsion and miniemulsion polymerizations and in this context has exhibited essentially ideal RAFT behavior.[43,46]

Materials and Methods

The RAFT agent, 2-{[(dodecylsulfanyl)carbonothioyl]sulfanyl}-propanoic acid (DoPAT) (>99.5% purity), was supplied by Dulux Australia (Victoria, Australia). One method used to prepare DoPAT has been described elsewhere.[46] AIBN was used as the initiator. Butyl acrylate (BA), butyl acetate, and AIBN were used as received from Sigma (>99% purity). Reactions were carried out with a total of ~27 mass % BA in butyl acetate in a 50 mL three-neck reactor under N_2 blanket at 70 °C.

ACOMP background, theory, and instrumentation have been described in detail previously.[58] The reactor was a 50 mL three-neck round-bottom reactor. Into one neck was inserted a condenser; the other two necks were sealed with rubber septa. A thermocouple and lines for N_2 purge and reactor liquid withdrawal were inserted through the septa. The reactor liquid was purged with N_2 before and throughout the reaction, and a small stream was withdrawn

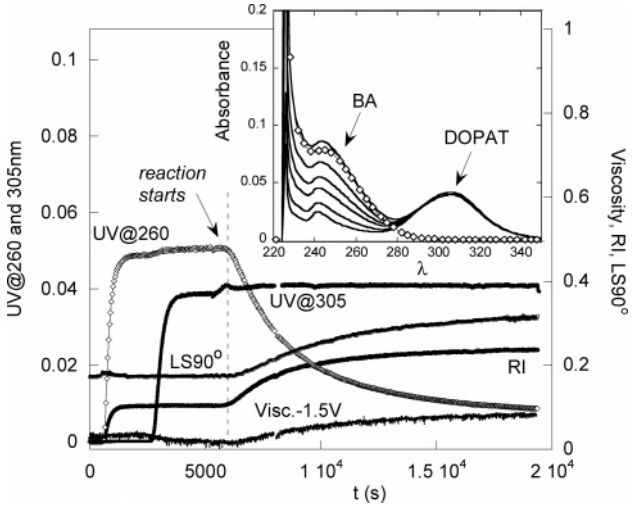

Figure 1. Raw ACOMP signals for viscometer, UV (at 260 and 305 nm), RI, and MALS at 90° scattering angle (data for seven angles were collected) (reaction 1, Table 1). The reaction starts when the initiator is added, as indicated. The inset shows a few selected UV spectra, which are collected every 2 s during the reaction.

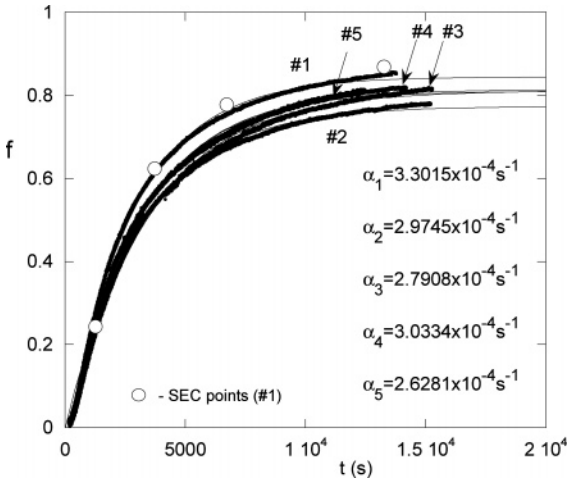

Figure 2. Conversion vs time for the reactions listed in Table 1. The discrete white circles are GPC results for aliquots from reaction 1.

continuously at 0.1 mL/min by a Shimadzu HPLC pump and further diluted before reaching the detector train. The ACOMP system used a five-pump system in order to achieve a two-stage dilution, one (5%) in a low-pressure mixing chamber pressure and the other (20%) in a high-pressure mixing chamber, yielding a 100-fold dilution. Each dilution stage was made with butyl acetate. The total detector flow rate was 2.0 mL/min, yielding ~0.0027 g/mL of total monomer concentration in the detector train.

Reactor fluid viscosity increased enough during some of the reactions that extraction efficiency of the HPLC pump was diminished but was taken into account accurately via the method of Florenzano et al.[58] This problem can be avoided by using the high-viscosity approach of Mignard et al.,[59] involving a gear pump for extraction from the reactor. Detectors comprised a Brookhaven Instruments Corp. (BI-MwA) multiangle light scattering photometer, a Shimadzu differential refractometer (RID-10A), a custom-built single capillary viscometer,[60] and a Shimadzu photodiode array UV/vis spectrophotometer (SPM-20A).

Automatic continuous mixing (ACM) was used to compute the second virial coefficient A_2 and to cross-check ACOMP values for M_w and $[\eta]_w$. The experiments were carried out with a Shimadzu gradient mixer and the same detector train as above, as previously described.[61]

Table 1. List of Experiments and Their Conditions[a]

no.	[BA]/[DoPAT]	[DoPAT]/[AIBN]	$M_{n,th}$ at $f = 1.0$	M_w at $f = 0.8$	M_w extrap at $f = 1$	M_w/M_{nth} at $f = 1$	A_2 (mol cm^3/g)	$\eta_{r,w}$ at $f = 0.8$	$\eta_{r,w}$ at $f = 1$	M_v at $f = 0.8$	M_v at $f = 1$
1	365.4	2.4	45100	32350	38600	0.86	6.28×10^{-4}	18.5	22.6	31400	39900
2	700	1.25	86400	51380	59800	0.69	5.91×10^{-4}	27.8	32.4	48900	58600
3	1693	0.51	2.09×10^5	1.16×10^5	1.41×10^5	0.67	5.44×10^{-4}	41.7	44.6	91100	1.04×10^5
4	7411	0.11	9.15×10^5	2.22×10^5	2.16×10^5	0.24	4.28×10^{-4}	66.9	75.2	2.11×10^5	2.13×10^5
5	no DoPAT	0		3.38×10^5	3.43×10^5		4.98×10^{-4}	99.5	94.3	3.05×10^5	2.76×10^5

[a] All the M_w and $\eta_{r,w}$ values are from ACOMP data. All the reactions were done at 70 °C, with AIBN as initiator, [AIBN] = 0.0024 M; and $[BA]_{in\ reactor}$ = 2.08 M. Analysis based on RI and UV260 signals.

Table 2. List of Parameters (Average and Standard Deviation from Five Experiments, Unless Otherwise Noted)[a]

$\partial n/\partial c_{BA}$	$\partial n/\partial c_{pBA}$	$\partial n/\partial c_{DoPAT}$	ϵ_{BA}, cm^2/g, at 260 nm	ϵ_{pBA}, cm^2/g, at 260 nm	ϵ_{DoPAT}, cm^2/g, at 260 nm
0.0242 ± 11%	0.084	0.0723 ± 3%	1463 ± 3%	0	5030 ± 11%

[a] The values for $\partial n/\partial c_{pBA}$ and ϵ_{pBA} were taken from other experiments.

Multidetector gel permeation chromatography (GPC) was used to determine molar mass distributions of end products and as an independent, conventional cross-check on fractional molar conversion f and M_w. GPC eluent, butyl acetate, was passed through the same detector train as in ACOMP and through columns using an LC-ATvp Shimadzu HPLC pump. The chromatographic columns were Polymer Labs PLgel Mixed B. The injector loop was 100 μL, and a flow rate of 0.8 mL/min was used. UV chromatograms at 250 nm were used in computing monomer conversion by integrating the peaks obtained by separation of the species eluted. The absolute molar mass of each elution slice was determined by combining the light scattering (MALS) with the concentration furnished by the RI data, so that no column calibration was used. Likewise, the intrinsic viscosity [η] of each slice was obtained from the capillary viscometer output voltage and the RI without recourse to any calibration.

A list of the various reactions, their conditions, theoretical final number-average mass M_n, etc., is given in Table 1, along with reaction end-point results from ACOMP and extrapolations of the ACOMP data to full conversion ($f = 1$). Table 2 shows the values of incremental refractive index values, dn/dc, for the monomer and polymer and UV extinction coefficients, ϵ. $\partial n/\partial c_{BA}$,$\partial n/\partial c_{DoPAT}$, $\epsilon_{BA@260}$, and $\epsilon_{DoPAT@260}$ were determined for each reaction, whereas $\partial n/\partial c_{pBA}$ and $\epsilon_{pBA@260}$ were computed from different sources.

Results

Figure 1 shows raw ACOMP signals from different detectors for a typical reaction (no. 1, Table 1). The increase of LS 90°, viscosity, and RI voltages after the addition of AIBN (at 6000 s) follows the growth of the polymer chains, whereas the decrease in UV (260 nm) follows the monomer consumption. Additionally, UV at 305 nm is used to monitor the evolution of the trithiocarbonate moiety during its transfer from DoPAT to a macroRAFT species and subsequent polymer growth from the latter. It may be possible to add a suitable detector for monitoring the disappearance of DoPAT during the intitialization step in future work.

The inset to Figure 1 shows the complete UV absorption spectra at selected points during conversion (spectra were collected every 2 s, as were all the other signals). The trithiocarbonate peak at 305 nm remains unchanged during the reaction, whereas the lower wavelengths dominated by BA decrease as conversion proceeds. This type of full spectrum capability will allow for monitoring RAFT copolymer synthesis. A recently introduced method allows computation of comonomer conversion in a model-independent fashion, using the superposition of basis spectra and error minimization.[62]

Figure 2 shows fractional monomer conversion f vs time for the reactions listed in Table 1. First-order functions fit the data well and are included in Figure 2, along with the numerical rates α for each reaction, where

$$f = 1 - e^{-\alpha t} \quad (1)$$

Data were determined using $\lambda = 260$ nm in conjunction with the RI data to track the efficiency of the pump withdrawing the sample stream from the reactor.

The first-order rates shown in the numerical inset to Figure 2 do not vary significantly with [DoPAT] over the concentration range studied here (from [DoPAT]/[AIBN] = 0 to 2.3). Hence, there is no evidence for retardation effects for this particular system. A consequence of this is that the quasi-steady-state approximation (QSSA),[63] which assumes that the rate of radical production equals the rate of radical disappearance throughout the reaction, should be applicable in this case.

This is similar to previous findings by Goto et al.,[64] in that the rate is essentially of zeroth order in [DoPAT] and depends almost solely on the initiator (AIBN) concentration. The literature is replete, however, with many RAFT systems in which rate retardation effects are prominent. The general trend for retarding RAFT agents is that increasing [RAFT] at fixed initiator concentration leads to increasing retardation (longer induction period and slower conversion).[51,65−67] This effect has also been found computationally using the method of moments approach.[68] Retardation involves complex sets of phenomena and depends on the RAFT agent/monomer chosen, concentrations, impurities, overall design of the experiment, etc.

Also shown as large circles in Figure 2 are GPC results on conversion for aliquots withdrawn from reaction 1 (UV at 250 nm was used to compute f from GPC data). When benzoyl peroxide (BPO) was substituted for AIBN, first-order conversion kinetics were again found, but the rate for BPO at the same molar concentration as AIBN and reaction temperature was 60% of that for AIBN. A peculiarity of the initial AIBN experiments was that when [AIBN] was 0.62 mM, the reaction stopped at partial conversion but restarted when more AIBN was added. The origin of this is not obvious, since the reaction stopped long before the half-life of the AIBN was reached: 7 h at 70 °C.[69]

Figure 3a gives the evolution of M_w with conversion for the same series of reactions. [AIBN] = 0.002 42 M was kept constant for all the reactions, but [DoPAT] was increased from zero in the top curve to [DoPAT] = 0.005 69 M in the bottom curve. The ratio [DOPAT]/[AIBN] is included in Table 1 and ranged from 0 to 2.4. M_w was computed on the basis of the extrapolation of Kc/I vs q^2 to $q = 0$. M_w data obtained were

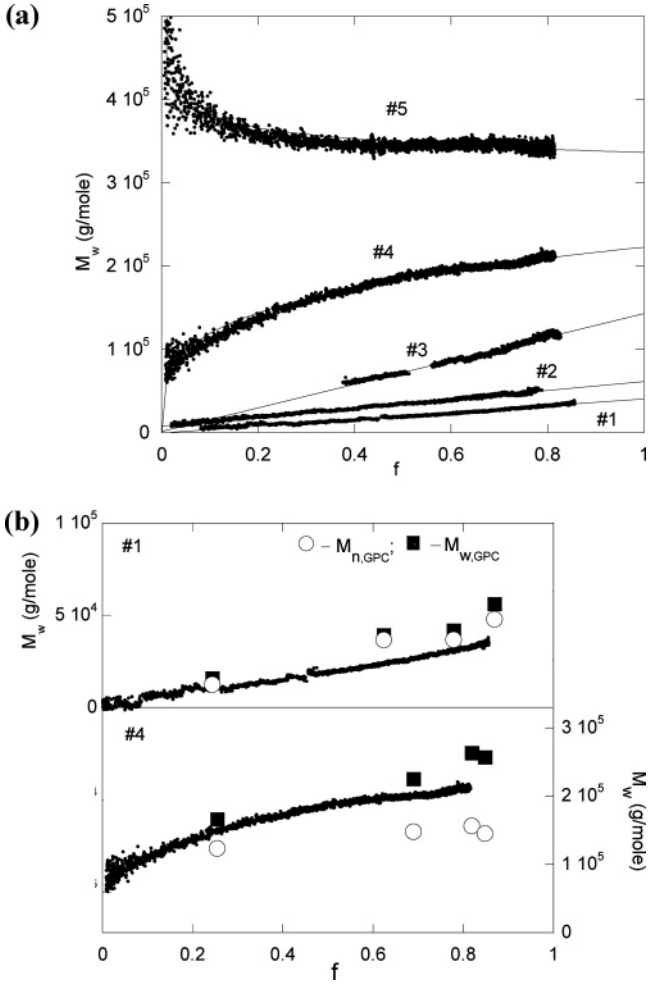

Figure 3. (a) M_w vs f from ACOMP for the five experiments in Table 1. The lines for the last 20% of conversion are just guides for the eye based on the experimental trends. (b**)** Enlargement of M_w vs f from ACOMP for experiments 1 and 4. Also shown are the GPC values of M_n and M_w for a few manually withdrawn aliquots for reactions 1 and 4. It is clear that the polydispersity of reaction 4 is much larger than for reaction 1.

then corrected for finite polymer concentration, using A_2 values determined in separate automatic continuous mixing (ACM) experiments. The values of A_2 are shown in Table 1. The ACM experiments also showed that, at the dilution level in the ACOMP detector train, the weight-averaged reduced viscosity $\eta_{r,w}$ is virtually identical to the weight-averaged intrinsic viscosity $[\eta]_w$.

The thin lines for each experiment in Figure 3a are just guides for the eye to bridge the last 20% of conversion and visualize approximately where the reactions will end at $f = 1$. The lines for reactions 1−3 are from linear fits, whereas for reactions 4 and 5 they are from power law fits, *with no model implied in any case*.

Figure 3b gives an enlarged view of M_w vs f from ACOMP for experiments 1 and 4, together with M_n and M_w values from multidetector GPC measurements made on manually withdrawn aliquots from reactions 1 and 4, shown by the discrete squares and circles. The M_w values are in fairly good agreement with the ACOMP values. The differences between M_w and M_n are much larger for experiment 4, which had less living character and hence higher polydispersity.

At high values of [DoPAT]/[AIBN] (bottom three curves in Figure 3a) the reactions most resemble "living" radical polymerizations with nearly linear increase of mass vs fractional

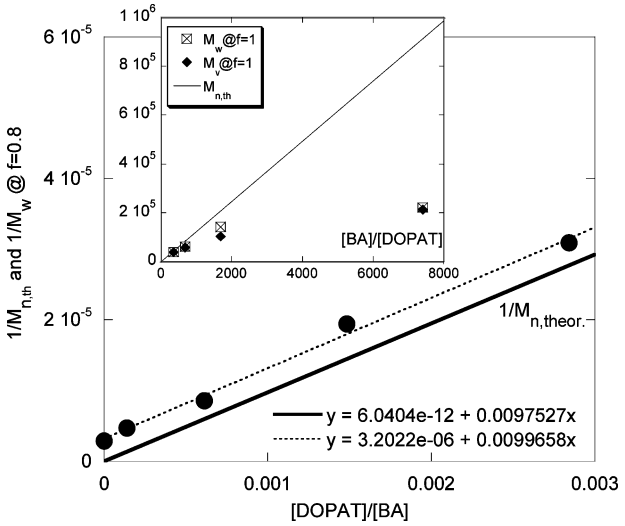

Figure 4. $1/M_w(f=0.8)$ vs $[\text{DoPAT}]_0/[\text{BA}]_0$ for reactions 1−5 are the solid circles, and the theoretical $1/M_n$ at $f = 0.8$ vs $[\text{DoPAT}]_0/[\text{BA}]_0$ is given by the solid line passing through the origin. Inset: squares and diamonds are respectively M_w and M_η vs $[\text{DoPAT}]_0/[\text{BA}]_0$, and $M_{n,th}$ vs $[\text{DoPAT}]_0/[\text{BA}]_0$ is the solid line passing through the origin.

monomer conversion f. For the lowest [DoPAT] experiment (no. 4) there is significant downward curvature of M_w vs f, showing very pronounced deviation from the ideal living mechanism. The top curve, for no DoPAT (no. 5), shows very typical uncontrolled radical polymerization behavior of M_w vs f, which is usually either constant or decreasing vs f. The downward curvature in no. 4 may be due to a transitional "hybrid behavior" stage where a significant fraction of polymer chains now grow by a conventional uncontrolled radical polymerization mechanism[70] and/or to transfer to solvent or monomer.

The polymerizations are seen to lead to values progressively under the theoretical value of $M_n = m_{BA}[\text{BA}]_0/[\text{DoPAT}]_0$. Figure 4 shows experimental values of $1/M_w$ vs $[\text{BA}]_0/[\text{DoPAT}]_0$at $f = 0.8$ conversion, and the solid line is the theoretical value of $1/M_n$ at $f = 0.8$. The inset to Figure 4 plots M_w (extrapolated to $f = 1$) and theoretical M_n at $f = 1$ vs $[\text{BA}]_0/[\text{DoPAT}]_0$. The direct M vs $[\text{BA}]_0/[\text{DoPAT}]_0$ shows more dramatically how far off the obtained values are from the theoretical values as [DoPAT] decreases.

Other points to note include the following:

(1) Except for reaction #1, M_w does not extrapolate to zero at $f = 0$, and $M_w(f = 0)$ increases as [DoPAT]/[BA] decreases. There are many experimental precedents for $M_n(f = 0) \neq 0$ in RAFT (if $M_n(f=0) = 0$, then $M_w(f=0)$ also),[71,72] including computational ones,[73] for which a direct extrapolation of actual experimental data to $f = 0$ will yield $M_n(f=0) \neq 0$. It is more commonly reported, however, that $M_n(f=0) = 0$.

(2) Concerning the large deviations between ideal and observed molar mass evolution, a preliminary analysis follows: By definition, M_n is the ratio of polymer concentration to the concentration of polymer chains. Considering that each RAFT agent ideally produces a propagating chain from its leaving group (R), the concentration of chains is equal to [DoPAT] plus chains produced by each AIBN decomposition reaction; M_n is then

$$M_n = m_{BA}\frac{f[\text{BA}]_0}{[\text{DoPAT}]_0 + dF[\text{AIBN}]_0\{1 - \exp(-k_d t)\}} \qquad (2)$$

where f is fractional monomer conversion, m_{BA} is the molar mass of BA, d is the number of chains produced per termination

reaction (= 1 for recombination, = 2 for disproportionation), F is the AIBN initiation efficiency, and k_d is the decomposition rate constant for AIBN, which is $\sim 2.75 \times 10^{-5}$ s^{-1} at T = 70 °C.

Equation 2 shows that as the ratio $[DOPAT]_0/[AIBN]_0$ increases the experimental values of M_n will approach the ideal "living" value, where the final value is $M_{n,th} = m_{BA}[BA]_0/[DOPAT]_0$. Table 1 includes $[DOPAT]_0/[AIBN]_0$ for each reaction as well as $M_{w,exp}/M_{n,th}$. There is a clear correlation that, as $[DOPAT]_0/[AIBN]_0$ increases, $M_{w,exp}/M_{n,th}$ approaches unity.

As a first approximation, $M_w \sim M_n$ for reactions with low polydispersity. Plotting $1/M_w(f=0.8)$ from Figure 3a and the theoretical $1/M_n$ at $f = 0.8$ is shown in Figure 4. The slope of $1/M_w(f=0.8)$ is remarkably close to that of $1/M_{n,theor}$ at $f = 0.8$, which is what is predicted by eq 2. The intercept yields $dF \sim 1.08 \pm 0.2$, taking into account the value of t at which $f = 0.8$ for experiments 1−5. While intriguing, this interpretation may be facile, since chain transfer reactions, to monomer, polymer, and solvent are ignored in the above expression. It was recently found in a study of the nitroxide-mediated polymerization of BA in butyl acetate at T = 118 °C that chain transfer to solvent was substantial and that $k_u/k_p = 0.000\,83$, where k_u and k_p are the transfer and propagation rate constants, respectively.[74] There was no evidence of transfer to monomer in that work.

If the concentration of dead chains, [Q], that are formed via radical transfer to monomer or other transfer agents, such as solvent, are also taken into account, then the above equation becomes, expressed in the conversion domain f

$$M_n(f) = \frac{f[BA]_0 m_{BA}}{[DoPAT]_0 + dF\{[AIBN]_0 - [AIBN](f)\} + \frac{k_{um}[BA]_0 f}{k_p + k_{um}} - \frac{k_u[T]}{k_p + k_{um}}\ln(1-f)} \quad (3)$$

where k_{um} is chain transfer constant to monomer and [T] is the concentration of transfer agent (T), and it is assumed that the [T] changes little during the reaction (e.g., T could be the solvent). It is noted that transfer to polymer will not change $M_n(f)$ since the number of chains does not change in that event. (Transfer of a radical to solvent or a transfer agent initiates a new chain, so that two chains emerge from the event, one dead and one propagating.) Equation 3 shows that transfer to monomer or other agents will cause even further reductions of M_n below the values predicted by eq 2. This equation could guide experiments aimed at testing the different mechanisms; e.g., bulk reactions would make [T] = 0, eliminating effects of transfer to solvent, whereas using solvent and varying $[m]_0$ can reveal if transfer to monomer is important, etc.

Figure 5 shows reduced viscosity $\eta_{r,w}$ vs f for the five reactions. As mentioned, these values are virtually identical to $[\eta]_w$. The same general trend as seen in Figure 3a is captured in Figure 5, which provides a good cross-check on the scattering data since the viscometer used for this determination is an independent detector.

GPC measurements yielded the following Mark−Houwink relationship for BA in butyl acetate at T = 25 °C:

$$[\eta] = 0.01209M^{0.722} \quad (4)$$

To obtain this, the GPC light scattering detector was used in conjunction with the RI to determine M of each elution slice in the GPC chromatogram; i.e., the absolute value of molar mass was obtained without any column calibration. Similarly, $[\eta]$ was determined directly with the GPC single capillary viscometer in conjunction with the RI, without any calibration required. The data for this determination are shown in Figure 6a and represent the combined GPC results for the five experiments.

The viscosity-averaged mass M_η for the ACOMP data was then obtained by replacing $[\eta]$ by $[\eta]_w$ and M by M_η in the

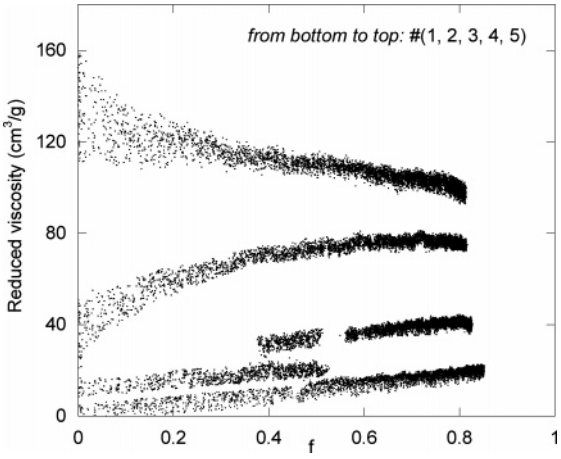

Figure 5. Reduced viscosity curves vs fractional monomer conversion (f) for the five reactions.

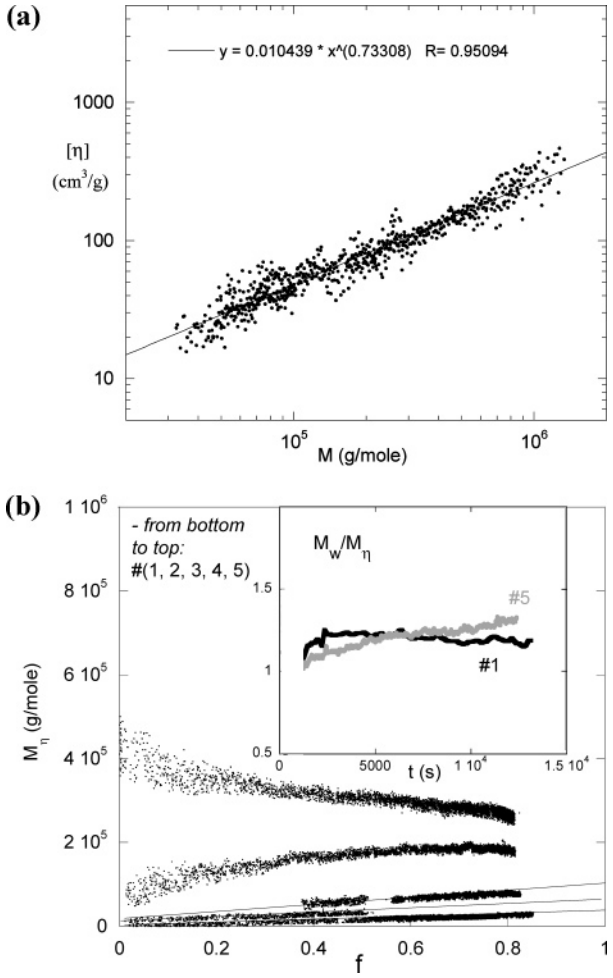

Figure 6. (a) GPC data from which the Mark−Houwink relationship ($[\eta]$ vs M) is found for pBA, as described in the text. **(**b**)** Viscosity averaged mass M_η as a function of conversion for all the experiments in Table 1, using the Mark−Houwink relationship from eq 4, whose values are from (a). Inset: M_w/M_η for reactions 1 and 5 serves as a measure of polydispersity.

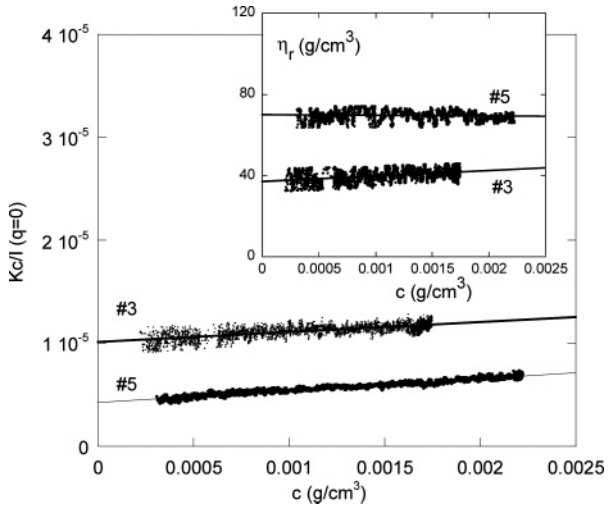

Figure 7. ACM results: $Kc/I(q=0)$ vs c for reactions 3 and 5. Inset: $\eta_{r,w}$ vs c result from ACM for the same reactions.

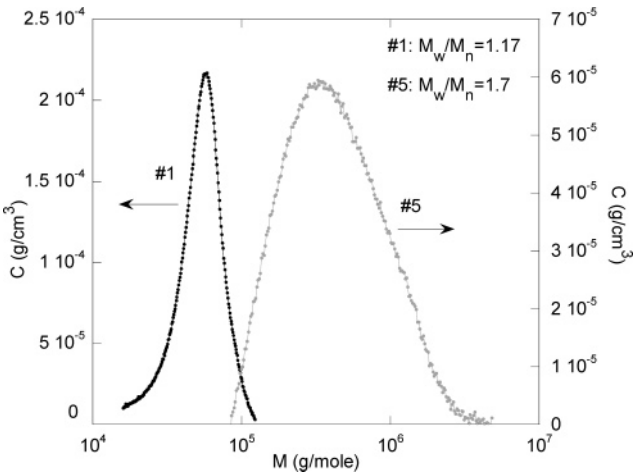

Figure 8. Complete molar mass distributions for the end products of reactions 1 and 5.

above relationship obtained by GPC. The results are shown in Figure 6b, where values very similar to those in Figure 3a are found. The quantity M_w/M_η is in itself a measure of polydispersity. With the above Mark−Houwink relationship, it is seen that M_η lies between M_n and M_w. There is a lot of noise when this ratio of values is taken, but the trend is nonetheless clear. The inset of Figure 6b shows M_w/M_η for the first and last experiments in Table 1; according to expectation, the ratio decreases somewhat for experiment 1, which is the most controlled, and increases for the uncontrolled radical polymerization.

ACM Results on End Products. As mentioned, ACM measurements provide the A_2 values needed for the small corrections to M_w at the finite concentrations in the ACOMP detector train. The same measurements also show the behavior of the directly measured $\eta_{r,w}$ to $[\eta]_w$. Figure 7 gives examples of ACM data for experiments 3 and 5. The values of $Kc/I(q=0)$ in Figure 7 involves the excess Rayleigh scattering ratio I (total scattering intensity minus scattering from solvent) at $q = 0$, obtained by extrapolation of the multiangle data to $q = 0$, and for vertically polarized incident light $K = (2\pi n\ \partial n/\partial c)^2/N_A\lambda^4$, where n is the index of refraction of the solvent, $\partial n/\partial c$ is the incremental refractive index for the polymer in the solvent, N_A is Avogadro's number, λ is the vacuum wavelength of the incident light, and c is the concentration of polymer in the detector train.

GPC Results on Molar Mass Distributions. GPC provides a valuable complement to ACOMP. In addition to the cross-check on conversion shown in Figure 2 using the GPC and ACOMP values, and obtaining the Mark−Houwink relationship above, GPC data show the expected trends for polydispersity; M_w/M_n is markedly lower for "living" polymerizations than for uncontrolled radical polymerizations, which is also consistent with the M_w/M_η data shown in the inset to Figure 5b.

Figure 8 shows the complete molar mass distributions for the end products of reactions 1 and 5 (M_w/M_n values are listed in the graph).

Summary

ACOMP was used to monitor the monomer conversion kinetics and evolution of M_w and η_r for RAFT polymerizations of BA in butyl acetate, using DoPAT as the RAFT agent. For fixed initiator concentration, [AIBN], monomer conversion was fit very well by first-order functions in time for all [DoPAT], including [DoPAT] = 0, and the rate was virtually independent of [DoPAT]; i.e., there was no evidence of RAFT agent induced retardation in this case. ACOMP should provide a powerful means of studying retardation and other kinetic effects for RAFT reactions.

Despite the nearly identical monomer conversion kinetics for all reactions, the crossover from "living" polymerizations at high [DoPAT] to hybrid behavior and then to uncontrolled polymerization as [DoPAT] decreased caused dramatic shifts in $M_w(f)$ and $\eta_{r,w}(f)$, even though all other reaction conditions were held identical. The coformation of chains produced by uncontrolled radical polymerization during this hybrid stage was responsible for the large deviations from ideal living behavior as [DoPAT] decreased and caused final $M_w(f=1)$ to be progressively lower than the theoretical values. It is difficult to separate evidence of conventional chain transfer processes from the definite presence of the coformation of uncontrolled polymer radical chains with the current data. ACOMP experiments in bulk would eliminate side reactions involving chain transfer to solvent, and other experiments can be designed to test other possible effects, such as transfer to monomer.

Trends in the independently measured η_r reflect those of $M_w(f)$ and also offer an index of polydispersity M_w/M_η, albeit a noisy one, which decreases for RAFT reactions at high RAFT agent and increases for low or no RAFT agent. Traditional multidetector GPC measurements substantiate conclusions concerning conversion kinetics and the expected trend for living reactions to have lower polydispersity than uncontrolled radical polymerizations.

This work clears the way for a more extensive use of ACOMP directed to the quantitative study of RAFT kinetics and mechanisms. There is clearly room for incorporating additional flow-through detectors, e.g. for identifying species that exist in low concentration. Near term ACOMP work will involve RAFT gradient and block copolymerization reactions and RAFT reactions in emulsions. Longer term goals include feedback control of RAFT processes, including multistage processes and development of "on-command" polymers of desired properties.

Acknowledgment. The authors acknowledge support from US National Science Foundation CBET 0623531, Louisiana Board of Regents ITRS-RD-B-05, NASA NCC3-9446, the Tulane Institute for Macromolecular Engineering and Science, and the Tulane Center for Polymer Reaction Monitoring and Characterization (PolyRMC).

References and Notes

(1) Matyjaszewski, K. Comparison and classification of controlled/living radical polymerizations. In Matyjaszewski, K., Ed. *Controlled/Living Radical Polymerization. Progress in ATRP, NMP, and RAFT*; ACS Symposium Series Vol. 768; American Chemical Society: Washington, DC, 2000; pp 2−26.
(2) Braunecker, W. A.; Matyjaszewski, K. *Prog. Polym. Sci.,* **2007**, *32*, 93.
(3) Arehart, S. V.; Matyjaszewski, K. *Macromolecules* **1999**, *32*, 2221.
(4) Hawker, C. J.; Bosman, A. W.; Harth, E. *Chem. Rev.* **2001**, *101*, 3661.
(5) (a) Wang, J. S.; Matyjaszewski, K. *J. Am. Chem. Soc.* **1995**, *117*, 5614. (b) Kato, M.; Kamigaito, M.; Sawamoto, M.; Higashimura, T. *Macromolecules* **1995**, *28*, 1721.
(6) Mignard, E.; Lutz, J.-F.; Matyjaszewski, F.; Guerret, O.; Reed, W. F. *Macromolecules* **2005**, *38*, 9556.
(7) Chiefari, J.; Chong, Y. K.; Ercole, F.; Krstina, J.; Jeffery, J.; Le Tam, P. T.; Mayadunne, R. T. A.; Meijs, G. F.; Moad, C. L.; Moad, G.; Rizzardo, E.; Thang, S. H. *Macromolecules* **1998**, *31*, 5559.
(8) Perrier, S.; Takolpuckdee, P. *J. Polym. Sci., Part A: Polym. Chem.* **2005**, *43*, 5347.
(9) Mayadunne, R. T. A.; Rizzardo, E. Mechanistic and Practical Aspects of RAFT Polymerization. In *Living and Controlled Polymerization: Synthesis, Characterization and Properties of the Respective Polymers and Copolymers*; Jagur-Grodzinski, J., Ed.; Nova Science Publishers: New York, 2005; p 65.
(10) Moad, G.; Solomon, D. H. *The Chemistry of Radical Polymerization*, 2nd ed.; Elsevier: Oxford, 2006; p 502.
(11) Moad, G.; Rizzardo, E.; Thang, S. H. *Aust. J. Chem.* **2006**, *59*, 669.
(12) Favier, A.; Charreyre, M.-T. *Macromol. Rapid Commun.* **2006**, *27*, 653.
(13) Lowe, A. B.; McCormick, C. L. *Prog. Polym. Sci.* **2007**, *32*, 283.
(14) Rizzardo, E.; Chen, M.; Chong, B.; Skidmore, M.; Thang, S. H. *Macromol. Symp.* **2007**, *248*, 104.
(15) Barner, L.; Davis, T. P.; Stenzel, M.; Barner-Kowollik, C. *Macromol. Rapid Commun.* **2007**, *28*, 539.
(16) McCormick, C. L.; Kirkland, S. E.; York, A. W. *J. Macromol. Sci., Part C: Polym. Rev.* **2006**, *46*, 421.
(17) McCormick, C. L.; Lowe, A. B. *Acc. Chem. Res.* **2004**, *37*, 312.
(18) Fournier, D.; Hoogenboom, R.; Thijs, H. M. L.; Paulus, R. M.; Schubert, U. S. *Macromolecules* **2007**, *40*, 915.
(19) Su, W.; Zhao, H.; Wang, Z.; Li, Y.; Zhang, Q. *Eur. Polym. J.* **2007**, *43*, 657.
(20) Zhou, J.; Wang, L.; Yang, Q.; Liu, Q.; Yu, H.; Zhao, Z. *J. Phys. Chem. B* **2007**, *111*, 5573.
(21) Moad, G.; Dean, K.; Edmond, L.; Kukaleva, N.; Li, G.; Mayadunne, R. T. A.; Pfaendner, R.; Schneider, A.; Simon, G.; Wermter, H. *Macromol. Symp.* **2006**, *233*, 170.
(22) Ding, P.; Zhang, M.; Gai, J.; Qu, B. *J. Mater. Chem.* **2007**, *17*, 1117.
(23) Hotchkiss, J. W.; Lowe, A. B.; Boyes, S. G. *Chem. Mater.* **2007**, *19*, 6.
(24) Xu, G.; Wang, Y.; Pang, W.; Wu, W.-T.; Zhu, Q.; Wang, P. *Polym. Int.* **2007**, *56*, 847.
(25) Yuan, K.; Li, Z.-F.; LÜ, L.-L.; Shi, X.-N. *Mater. Lett.* **2007**, *61*, 2033.
(26) Zhao, Y.; Perrier, S. *Macromol. Symp.* **2007**, *248*, 94.
(27) Iwasaki, Y.; Takamiya, M.; Iwata, R.; Yusa, S.; Akiyoshi, K. *Colloids Surf., B* **2007**, *57*, 226.
(28) Kiani, K.; Hill, D. J. T.; Rasoul, F.; Whittaker, M.; Rintoul, L. *J. Polym. Sci., Part A: Polym. Chem.* **2007**, *45*, 1074.
(29) Narain, R.; Gonzales, M.; Hoffman, A. S.; Stayton, P. S.; Krishnan, K. M. *Langmuir* **2007**, *23*, 6299.
(30) Hawkett, B. S.; Such, C. H.; Nguyen, D. N.; Farrugia, J. M.; MacKinnon, O. M. PCT Int. Appl. WO 2006037161 A1 20060413.
(31) Skaff, H.; Emrick, T. *Angew. Chem., Int. Ed.* **2004**, *43*, 5383.
(32) McCormick, C. L.; Kirkland, S. E.; York, A. W. *J. Macromol. Sci., Part C: Polym. Rev.* **2006**, *46*, 421.
(33) Cheng, C.; Khoshdel, E.; Wooley, K. L. *Macromolecules* **2007**, *40*, 2289.
(34) Ge, Z.; Cai, Y.; Yin, J.; Zhu, Z.; Rao, J.; Liu, S. *Langmuir* **2007**, *23*, 1114.
(35) Ge, Z.; Xie, D.; Chen, D.; Jiang, X.; Zhang, Y.; Liu, H.; Liu, S. *Macromolecules* **2007**, *40*, 3538.
(36) Luo, Y.; Gu, H. *Polymer* **2007**, *48*, 3262.
(37) Bernard, J.; Hao, X.; Davis, T. P.; Barner-Kowollik, C.; Stenzel, M. H. *Biomacromolecules* **2006**, *7*, 232.
(38) Housni, A.; Cai, H.; Liu, S.; Pun, S. H.; Narain, R. *Langmuir* **2007**, *23*, 5056.
(39) Al-Bagoury, M.; Bucholz, K.; Yaacoub, E.-J. *Polym. Adv. Technol.* **2007**, *18*, 313.
(40) Özyürek, Z.; Komber, H.; Gramm, S.; Schmaljohann, D.; Müller, A. H. E.; Voit, B. *Macromol. Chem. Phys.* **2007**, *208*, 1035.
(41) Ting, S. R. S.; Granville, A. M.; Quémener, D.; Davis, T. P.; Stenzel, M. H.; Barner-Kowollik, C. *Aust. J. Chem.* **2007**, *60*, 405.
(42) Nicolas, J.; Mantovani, G.; Haddleton, D. M. *Macromol. Rapid Commun.* **2007**, *28*, 1083.
(43) Such, C. H.; Rizzardo, E.; Serelis, A. K.; Hawkett, B. S.; Gilbert, R. G.; Ferguson, C. J.; Hughes, R. J. PCT Int. Appl. WO 2003055919 A1 20030710.
(44) Ferguson, C. J.; Hughes, R. J.; Pham, B. T. T.; Hawkett, B. S.; Gilbert, R. G.; Serelis, A. K.; Such, C. H. *Macromolecules* **2002**, *35*, 9243.
(45) Pham, B. T. T.; Nguyen, D.; Ferguson, C. J.; Hawkett, B. S.; Serelis, A. K.; Such, C. H. *Macromolecules* **2003**, *36*, 8907.
(46) Ferguson, C. J.; Hughes, R. J.; Nguyen, D.; Pham, B. T. T.; Gilbert, R. G.; Serelis, A. K.; Such, C. H.; Hawkett, B. S. *Macromolecules* **2005**, *38*, 2191.
(47) McLeary, J. B.; Klumperman, B. *Soft Matter* **2006**, *2*, 45.
(48) Buttè, A.; Peklak, A. D.; Storti, G.; Morbidelli, M. *Macromol. Symp.* **2007**, *248*, 168.
(49) Bowes, A.; McLeary, J. B.; Sanderson, R. D. *J. Polym. Sci., Part A: Polym. Chem.* **2007**, *45*, 588.
(50) dos Santos, A. M.; Pohn, J.; Lansalot, M.; D'Agosto, F. *Macromol. Rapid Commun.***2007**, *28*, 1325.
(51) Barner-Kowollik, C.; Buback, M.; Charleux, B.; Coote, M. L.; Drache, M.; Fukuda, T.; Goto, A.; Klumperman, B.; Lowe, A. B.; McLeary, J. B.; Moad, G.; Monteiro, M. J.; Sanderson, R. D.; Tonge, M. P.; Vana, P. *J. Polym. Sci.* **2006**, *44*, 5809.
(52) Moad, G.; Rizzardo, E.; Thang, S. H. *Aust. J. Chem.* **2005**, *58*, 379.
(53) Mayadunne, R. T. A.; Rizzardo, E.; Chiefari, J.; Krstina, J.; Moad, G.; Postma, A.; Thang, S. H. *Macromolecules* **2000**, *33*, 243.
(54) Chernikova, E. V.; Terpugova, P. S.; Garina, E. S.; Golubev, V. B. *J. Polym. Sci., Ser. A* **2007**, *49*, 108.
(55) Chiefari, J.; Mayadunne, R. T. A.; Moad, C. L.; Moad, G.; Rizzardo, E.; Postma, A.; Skidmore, M. A.; Thang, S. H. *Macromolecules* **2003**, *36*, 2273.
(56) Theis, A.; Feldermann, A.; Charton, N.; Davis, T. P.; Stenzel, M. H.; Barner-Kowollik, C. *Polymer* **2005**, *46*, 6797.
(57) Postma, A.; Davis, T. P.; Evans, R. A.; Li, G.; Moad, G.; O'Shea, M. S. *Macromolecules* **2006**, *39*, 5293.
(58) Florenzano, F. H.; Strelitzki, R.; Reed, W. F. *Macromolecules* **1998**, *31*, 7226.
(59) Mignard, E.; Leblanc, T.; Bertin, D.; Guerret, O.; Reed, W. F. *Macromolecules* **2004**, *37*, 966.
(60) Norwood, D. P.; Reed, D. P. *Int. J. Polym. Anal. Charact.* **1997**, *4*, 99.
(61) Sorci, G. A.; Reed, W. F. *Macromolecules* **2002**, *35*, 5218.
(62) Alb, A. M.; Enohnyaket, P.; Drenski, M. F.; Head, A.; Reed, A. W.; Reed, W. F. *Macromolecules* **2006**, *39*, 8283.
(63) Dotson, N. A.; Galvan, R.; Laurence, R.; Tirrel, M. *Polymerization Process Modelling*; VCH Pub.: New York, 1996.
(64) Goto, A.; Sato, K.; Tsujii, Y.; Fukuda, T.; Moad, G.; Rizzardo, E.; Thang, S. H. *Macromolecules* **2001**, *34*, 402.
(65) Prescott, S. W.; Ballard, M. J.; Rizzardo, E.; Gilbert, R. G. *Macromolecules* **2005**, *38*, 4901.
(66) Chernikova, E.; Morozov, A.; Leonova, E.; Garina, E.; Golubev, V.; Bui, C.; Charleux, B. *Macromolecules* **2004,** *37*, 6329.
(67) Feldermann, A.; Ah Toy, A.; Davis, T. P.; Stenzel, M. H.; Barner-Kowollik, C. *Polymer* **2005**, *46*, 8448.
(68) Wang, A. R.; Zhu, S. *J. Polym. Sci., Part A: Polym. Chem.* **2003**, *41*, 1553.
(69) Smiley, R. A.; Mark, H. F.; Othmer, D. F.; Overberger, C. G. In *Kirk-Othmer Encyclopedia of Chemical Technology*, 3rd ed.; John Wiley and Sons: New York, 1981; Vol. 15; pp 889−909.
(70) Barner-Kowollik, C.; Quinn, F. J.; Nguyen, T. L. U.; Heuts, J. P. A.; Davis, T. P. *Macromolecules* **2001**, *34*, 7849.
(71) Yang, C.; Cheng, Y.-L. *J. Appl. Polym. Sci.* **2006**, *102*, 1191.
(72) An, Q.; Qian, J.; Yu, L.; Luo, Y.; Liu, X. *J. Polym. Sci., Part A: Polym. Chem.* **2005**, 1973.
(73) Litvinenko, G.; Mueller, A. H. E. *Macromolecules* **1997**, *30*, 1253.
(74) Drenski, M. F.; Mignard, E.; Reed, W. F. *Macromolecules* **2006**, *39*, 8213.

MA071579P